Supporting Information

Two-dimensional metal $NaCu_{6.3}Sb_3$ and Solid-Solid Transformations for Sodium Copper Antimonides

*Bryan Owens-Baird, Shannon Lee, and Kirill Kovnir**

Experimental

Powder X-ray Diffraction

Samples were analyzed via room-temperature powder X-ray diffraction using a Rigaku Miniflex 600 diffractometer employing Cu-K_α radiation (λ = 1.54185 Å) with a Ni-K_β filter. Scans were performed from 5 – 80° 2θ on a spinning sample Si-crystal zero-background plate.

Variable Temperature Synchrotron Powder X-ray Diffraction

Variable temperature PXRD data was collected at the synchrotron beamline: 17-BM at the Advanced Photon Source (APS) at Argonne National Lab (ANL). Laboratory prepared samples were loaded into 0.5 mm inner diameter silica capillaries (0.7 mm outer diameter) and sealed under vacuum. The sealed silica capillaries were placed into a secondary shield capillary, with a thermocouple set as close as possible to the measurement area. An experimental set-up can be found elsewhere.[1] The data was collected with λ = 0.45336 Å and a temperature range from 300 K to 1073 K.

Single-Crystal X-ray Diffraction

Single-Crystal X-ray Diffraction was carried out using a Bruker D8 Venture diffractometer with a Bruker Photon100 CMOS detector and employing Mo-K_α radiation (λ = 0.71073 Å). The dataset was collected at 100 K under a N_2 stream with a variety of φ- and ω-scans recorded at a 0.3° step and integrated using the Bruker SAINT software package.[2] Multiscan absorption correction was used on the data. Structure solution and refinement was achieved using the SHELX suite.[3] Atomic positions, occupancy, and atomic displacement parameters are shown in Table 1. Full details of the structure refinement, selected interatomic distances and angles, and anisotropic displacement parameters can be found in Tables S1-S3.

At the final stages of the refinement, high residual electron density peaks and extremely large anisotropic displacement in the [001] plane were observed for Sb(1) atoms located at the 2*b* special position (0,0,¼). This position was allowed to relax to 6*h* position with coordinates (*x*,2*x*,¼) with occupancy fixed to 33.3%. This shift resulted in the elimination of high difference electron density peaks and a twofold drop in the R_1/wR_2 values. Sb(1) located in the 6*h* position created a threefold position with 0.25 Å separation (Figure S6). The interatomic separations between Cu(4) and Sb(1) are 2.288(9) Å and 2.511(8) Å. While 2.511 Å is similar to other reported Cu-Sb distances, 2.288 Å is too short to be

real. We hypothesize that the split of Sb(1) position is caused by presence of the vacancies in the surrounding Cu(4) sites.

Energy Dispersive X-ray Spectroscopy

Elemental composition analysis was performed through Energy Dispersive X-ray Spectroscopy using a Hitachi S4100 T SEM (Oxford INCA energy). For each composition, measurements were taken at a collection of sites on multiple crystals to improve statistics.

Differential Scanning Calorimetry

Differential Scanning Calorimetry was performed using a Netzsch Thermal Analysis STA 409 calorimeter. Approximately 30 mg of sample was loaded and sealed in small evacuated silica ampoules and measured between 323-1073 K with a heating/cooling rate of 10 K/min.

Sample Densification

Pellets of $NaCu_{6.3}Sb_3$ and $NaCu_4Sb_2$ for property measurements were prepared by use of an 8-mm stainless steel die. Finely ground powders were cold pressed with a force of 7 MPa, yielding shiny metallic pellets. Ingots of Cu_2Sb were used as prepared from synthesis and cut into regular shapes. The pelletized samples of Cu_2Sb, $NaCu_{6.3}Sb_3$, and $NaCu_4Sb_2$ had geometrical densities of 90%, 95%, and 92% of their theoretical X-ray densities, respectively. Purity of the samples was confirmed through PXRD.

Physical Properties

Thermal and charge-transport properties were measured from 10-300 K using a Quantum Design Physical Property Measurement System. The Seebeck thermopower and thermal conductivity were measured using the Thermal Transport Option in a two-probe configuration. Electrical resistivity was measured using the Alternating Current Transport option and a four-probe geometry with 50 μm platinum wires and silver paste. Partial degradation of the samples would occur if measured to the instrument temperature limit of 400 K.

Band Structure Calculations

Band structure and density of state data was calculated using the tight binding linear muffin-tin orbital, atomic sphere approximation (TB-LMTO-ASA) program.[4] Experimentally obtained lattice parameters and atomic positions were used in the calculations. The band structures and density of states were calculated after a converging of the total energy. Two models were used to calculate the electronic structure of $NaCu_{6.3}Sb_3$: fully occupying or removing the Cu(4) site, yielding compositions of $NaCu_7Sb_3$ and $NaCu_6Sb_3$, correspondingly. In both models the idealized position 2*b* (0,0,¼) for Sb(1) was used. The density of *k*-mesh for Cu_2Sb, $NaCu_6Sb_3$, $NaCu_7Sb_3$, and $NaCu_4Sb_2$ was 16×16×25, 42×42×14, 42×42×14, and 50×50×8, respectively. The number of the irreducible *k*-points in the irreducible part of the Brillouin zone was 585, 1352, 1352, and 5101, respectively.

Table S1. Single crystal data and refinement parameters for $NaCu_{6.3}Sb_3$ at 100 K.

empirical formula	$NaCu_{6.35}Sb_3$
CSD-number	433160
formula weight	791.40 g/mol
temperature	100(2) K
radiation, wavelength	Mo-K_α, 0.71073 Å
crystal system	Hexagonal
space group	$P6_3/mmc$ (No. 194)
unit cell dimensions	a = 4.2166(2) Å
	c = 24.041(1) Å
unit cell volume	370.17(4) Å^3
Z	2
Data/parameters	263/23
density (calc.)	7.100 g/cm^3
absorption coefficient	28.551 mm^{-1}
R_{int}	0.036
goodness-of-fit	1.22
final R indices [$I > 2\sigma(I)$]	R_1 = 0.0218
	wR_2 = 0.0485
final R indices [all data]	R_1 = 0.0223
	wR_2 = 0.0490
largest peak and hole	1.935/-1.263 e Å^{-3}

Further details of the crystal structure may be obtained from FIZ Karlsruhe, 76344 Eggenstein-Leopoldshafen, Germany, crysdata@fiz-karlsruhe.de, on quoting the deposition number CSD-433160.

Table S2. Anisotropic displacement parameters ($Å^2$) for $NaCu_{6.3}Sb_3$ at 100 K.*

Atom	U_{11}	U_{22}	U_{33}	U_{12}	U_{13}	U_{23}
Na	0.011(1)	0.011(1)	0.006(2)	0	0	0.005(1)
Cu(1)	0.003(1)	0.003(1)	0.035(1)	0	0	0.002(1)
Cu(2)	0.015(1)	0.015(1)	0.002(1)	0	0	0.007(1)
Cu(3)	0.004(1)	0.004(1)	0.006(1)	0	0	0.002(1)
Cu(4)	0.005(1)	0.005(1)	0.008(1)	0	0	0.002(1)
Sb(1)	0.040(5)	0.013(1)	0.003(1)	0	0	0.020(2)
Sb(2)	0.004(1)	0.004(1)	0.002(1)	0	0	0.002(1)

*The anisotropic displacement factor exponent takes the form: $-2\pi^2[h^2a^{*2}U_{11} + \ldots + 2hka^*b^*U_{12}]$.

Table S3. Selected bond lengths (Å) and angles (°) from the structure of $NaCu_{6.3}Sb_3$ taken at 100 K.

Bond Length (Å)		Bond Angle (°)	
Cu(1)-Cu(3)	2.4346(1)	Cu(4)-Sb(1)-Cu(4)	114.2(4)/122.9(2)
Cu(1)-Sb(2)	2.728(1)	Cu(1)-Cu(3)-Cu(1)	119.990(1)
Cu(3)-Sb(2)	2.7168(4)	Cu(1)-Sb(2)-Cu(1)	101.22(3)
Cu(4)-Sb(1)	2.288(9)/2.511(5)	Cu(1)-Sb(2)-Cu(3)	126.82(3)
Sb(1)-Cu(2)	2.688(4)	Sb(1)-Cu(2)-Sb(1)	103.3(2)
Cu(2)-Sb(2)	2.584(1)	Sb(1)-Cu(2)-Cu(4)	123.8(1)
Cu(2)-Cu(1)	2.785(1)	Sb(2)-Na-Sb(2)	80.98(1)
Cu(2)-Cu(3)	2.798(1)	Sb(2)-Na-Sb(2)	99.02(1)
Na-Sb(2)	3.247(1)	Sb(2)-Na-Sb(2)	180.00(1)
Na-Na	4.216(1)	Sb(1)-Cu(2)-Sb(2)	130.04(7)
*Sb(1)-Sb(1)**	0.25(2)	Sb(1)-Sb(1)-Sb(1)	60.00(1)

*The Sb(1)-Sb(1) is not a distance present within the structure, but shows the distance between the three possible Sb(1) positions.

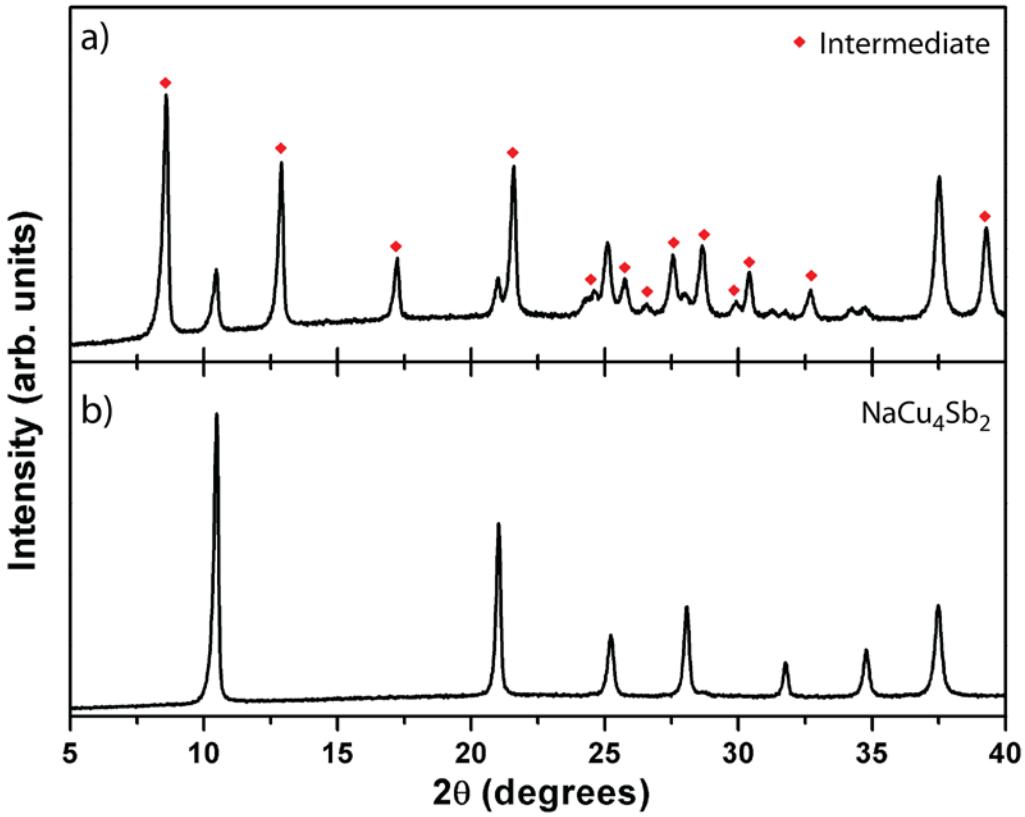

Figure S1. PXRD patterns of: (a) sample containing the intermediate phase and $NaCu_4Sb_2$, and (b) single-phase sample of $NaCu_4Sb_2$. Peaks assigned to the intermediate phase are labeled with red diamonds. All labeled peaks were indexed using the unit cell parameters obtained from single-crystal indexing and using the CMPR software package[5]: primitive hexagonal unit cell with a = 7.334 Å and c = 20.445 Å.

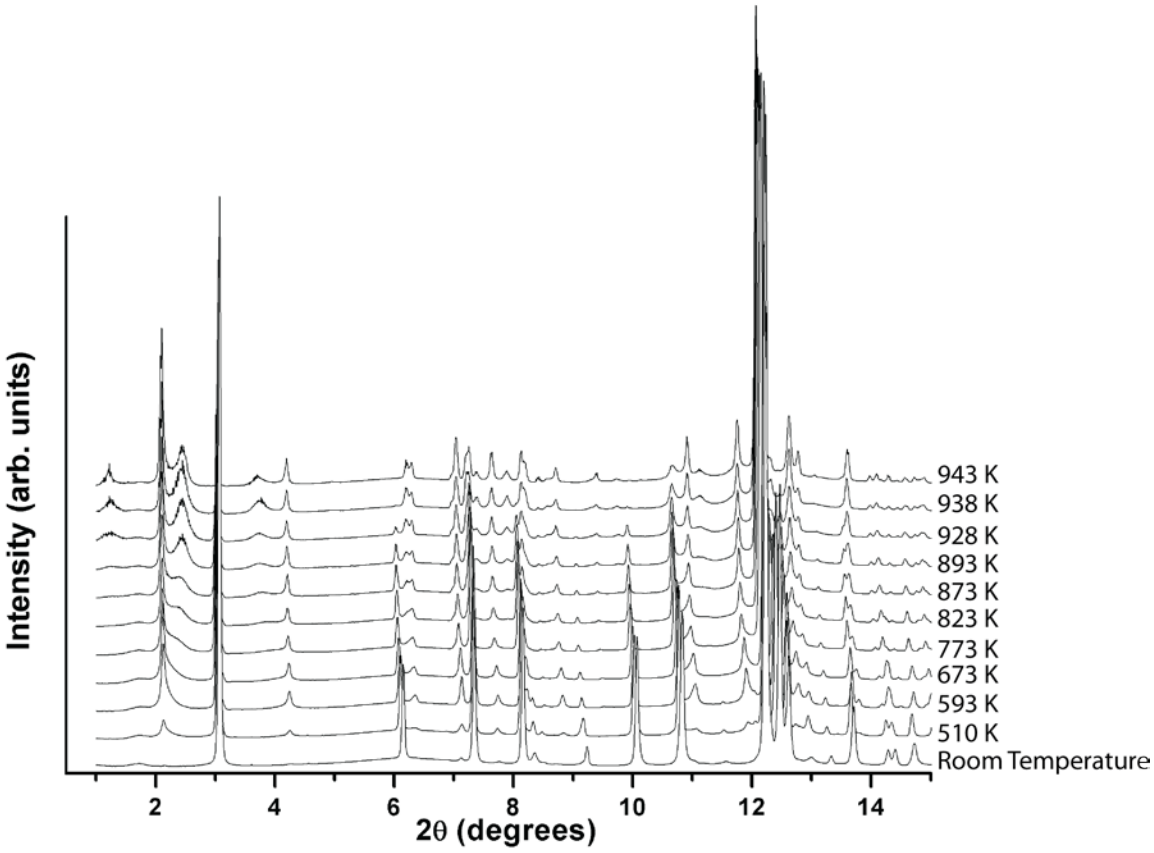

Figure S2. *In-situ* variable temperature synchrotron PXRD of $NaCu_4Sb_2$. The sample is heated from room temperature (bottom pattern) to 943 K (top pattern).

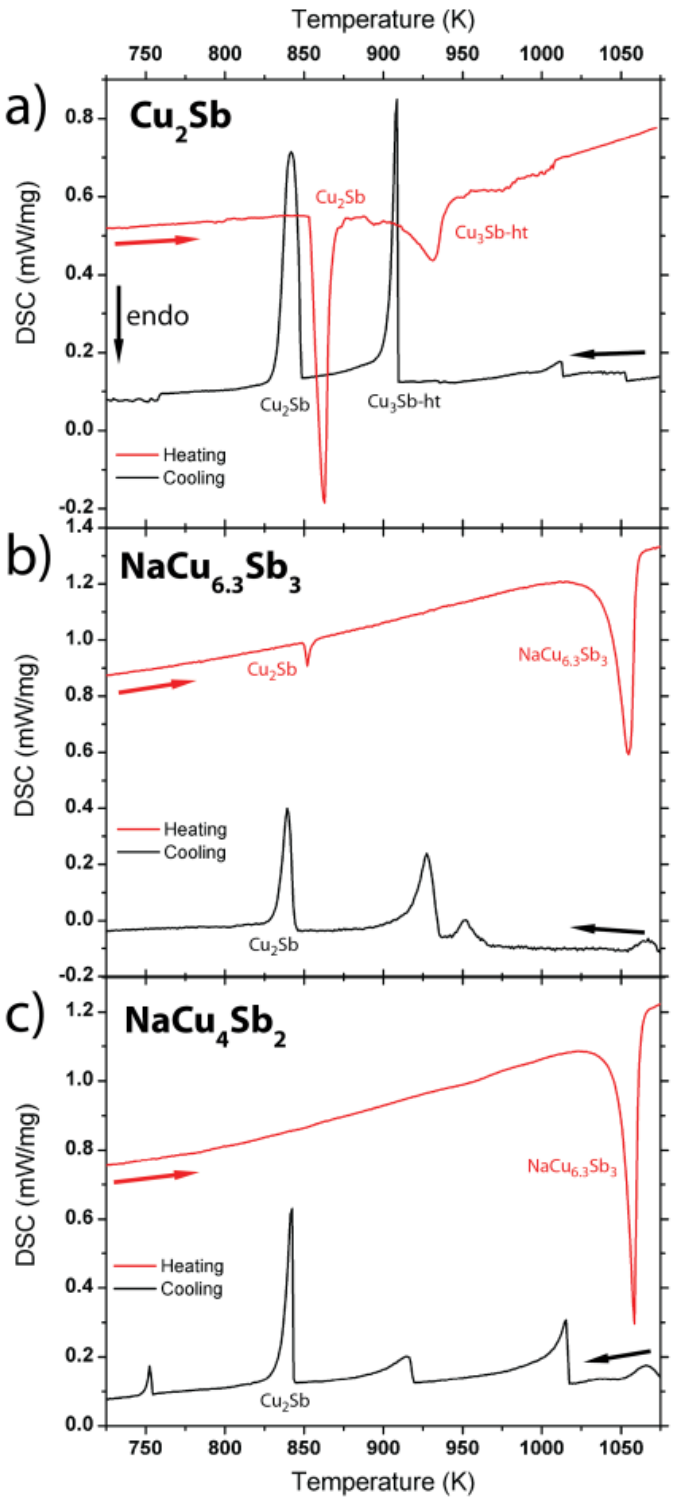

Figure S3. DSC plots for: (a) Cu_2Sb, (b) $NaCu_6Sb_3$, and (c) $NaCu_4Sb_2$. The arrows indicate the direction of measurement.

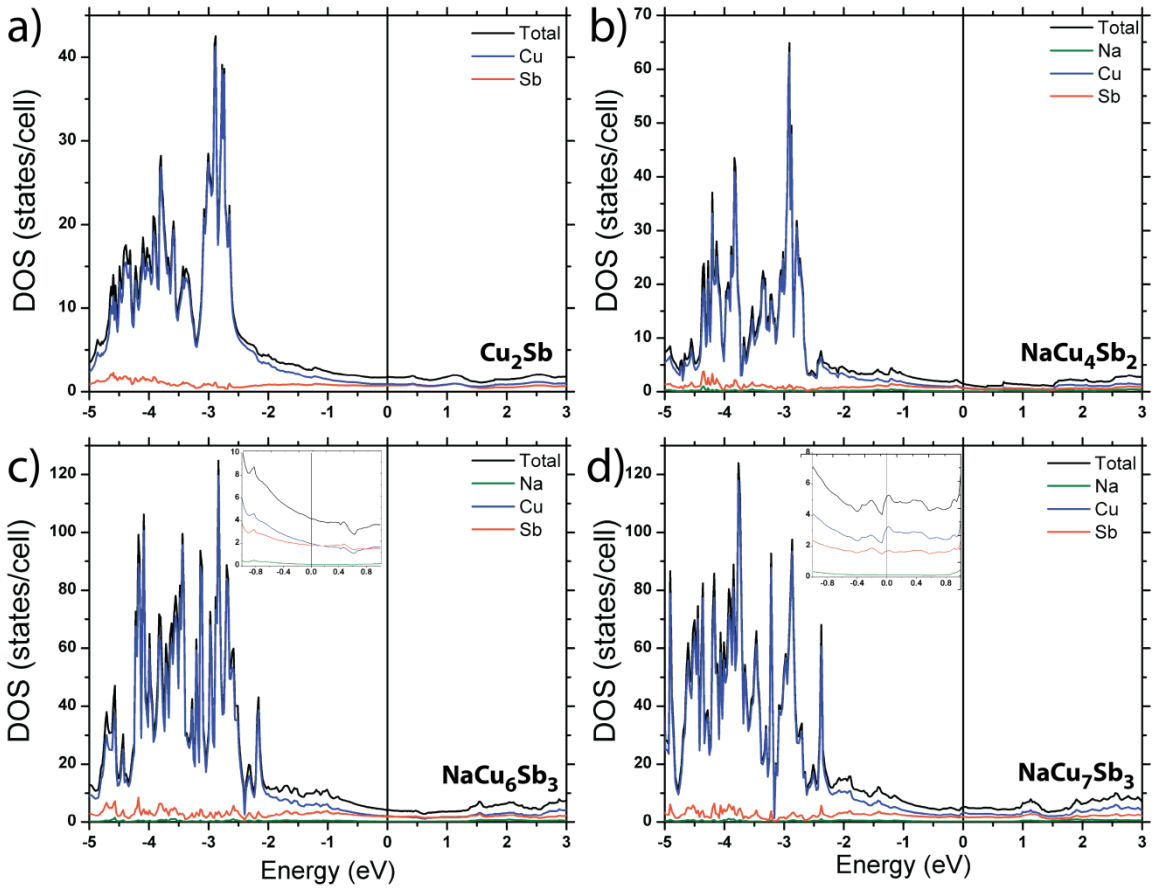

Figure S4. Density of states plots for: (a) Cu_2Sb, (b) $NaCu_4Sb_2$, (c) $NaCu_6Sb_3$ model, and (d) $NaCu_7Sb_3$ model. Insets of (c) and (d) show a zoom in near the Fermi level.

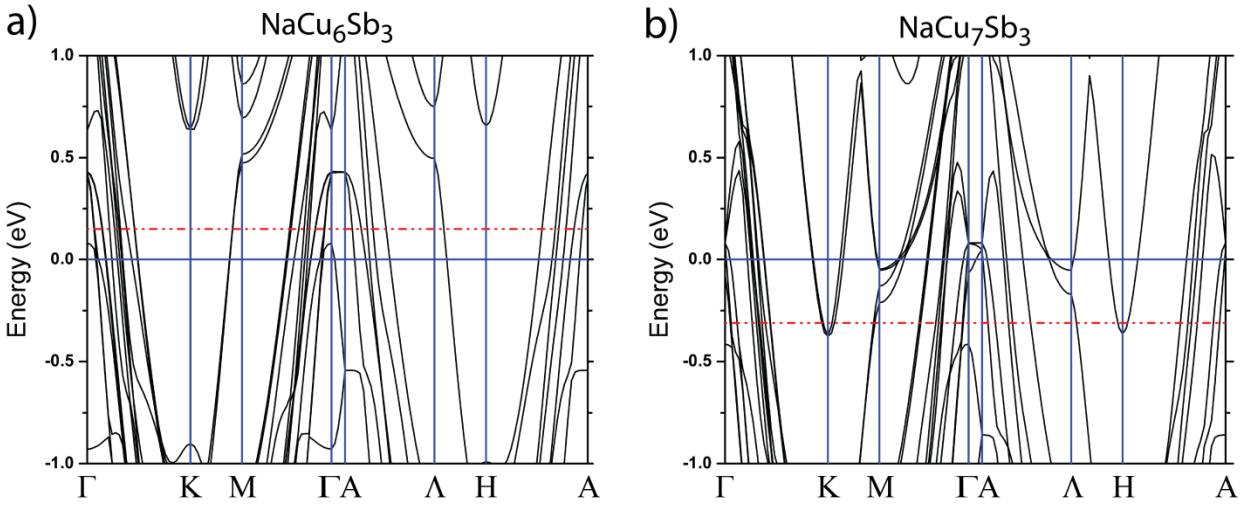

Figure S5. Calculated electronic band structure of: a) $NaCu_6Sb_3$ model and b) $NaCu_7Sb_3$ model. The dashed red line indicates the electron count for $NaCu_{6.3}Sb_3$.

References

(1) P.J. Chupas, K.W. Chapman, C. Kurtz, J.C. Hanson, P.L. Lee, C.P. Grey, *J. Appl. Cryst.* **2008**, 41, 822-824.

(2) SMART and SAINT. Bruker AXS Inc.: Madison, WI, USA, **2007**.

(3) Sheldrick, G. *Acta Crystallogr. Sect. A* **2008**, 64, 112.

(4) Jepsen, O.; Burkhardt, A.; Andersen, O. K. TB-LMTO-ASA **1999**, Version 4.7; Max-Plank-Institut für Festkörperforschung: Stuttgart, Germany.

(5) Toby, B., *Journal of Applied Crystallography*, **2005,** 38(6): p. 1040-1041.